



Since January 2020 Elsevier has created a COVID-19 resource centre with free information in English and Mandarin on the novel coronavirus COVID-19. The COVID-19 resource centre is hosted on Elsevier Connect, the company's public news and information website.

Elsevier hereby grants permission to make all its COVID-19-related research that is available on the COVID-19 resource centre - including this research content - immediately available in PubMed Central and other publicly funded repositories, such as the WHO COVID database with rights for unrestricted research re-use and analyses in any form or by any means with acknowledgement of the original source. These permissions are granted for free by Elsevier for as long as the COVID-19 resource centre remains active.



Full-length Article

CXCL13 promotes isotype-switched B cell accumulation to the central nervous system during viral encephalomyelitis



Timothy W. Phares^a, Krista D. DiSano^{a,b}, Stephen A. Stohlman^a, Benjamin M. Segal^c,
Cornelia C. Bergmann^{a,*}

^a Department of Neurosciences NC30, Lerner Research Institute, Cleveland Clinic Foundation, 9500 Euclid Avenue, Cleveland, OH, USA

^b School of Biomedical Sciences, Kent State University, Kent, OH, USA

^c Department of Neurology, University of Michigan Medical School, Ann Arbor, MI, USA

ARTICLE INFO

Article history:

Received 16 November 2015

Received in revised form 13 January 2016

Accepted 16 January 2016

Available online 18 January 2016

Keywords:

Central nervous system

Neuroimmunology

CXCL13

B cells

Antibody secreting cells

Memory B cells

ABSTRACT

Elevated CXCL13 within the central nervous system (CNS) correlates with humoral responses in several neuroinflammatory diseases, yet its role is controversial. During coronavirus encephalomyelitis CXCL13 deficiency impaired CNS accumulation of memory B cells and antibody-secreting cells (ASC) but not naïve/early-activated B cells. However, despite diminished germinal center B cells and follicular helper T cells in draining lymph nodes, ASC in bone marrow and antiviral serum antibody were intact in the absence of CXCL13. The data demonstrate that CXCL13 is not essential in mounting effective peripheral humoral responses, but specifically promotes CNS accumulation of differentiated B cells.

© 2016 Elsevier Inc. All rights reserved.

1. Introduction

The lymphoid chemokines CXCL12, CXCL13, CCL19 and CCL21 all regulate migration and compartmentalization of B cells within secondary lymphoid organs under homeostatic as well as activation/inflammatory conditions (Cyster, 2005; Okada and Cyster, 2006). In lymphoid organs CXCL13 is expressed in B cell follicles and contributes to germinal center (GC) formation by recruiting activated B and follicular helper CD4⁺ T (T_{fh}) cells expressing its cognate receptor CXCR5 (Victoria and Nussenzweig, 2012; Zotos and Tarlinton, 2012; Crotty, 2012). Formation of GC by coordinated chemokine engagement of CD4⁺ T cells and activated B cells in turn is critical for B cell differentiation, isotype switching and affinity maturation leading to antibody secreting cells (ASC) or memory B cells (B_{mem}) not secreting antibody (Ab). Both ASC and B_{mem} surviving selection in GCs exit and provide long-lived humoral immunity following infection or vaccination. While ASC comprise

long-lived plasma cells and their precursor plasma blasts, B_{mem} require antigen or innate re-stimulation to differentiate into ASC.

CXCL13 is also associated with lymphoid neogenesis and propagation of humoral responses in non-lymphoid tissue during chronic inflammatory diseases, such as rheumatoid arthritis, *Helicobacter pylori* gastritis, multiple sclerosis (MS) and primary central nervous system (CNS) lymphoma (Wengner et al., 2007; Finch et al., 2013; Rubenstein et al., 2013; Winter et al., 2010; Fischer et al., 2009). In MS patients, CXCL13 is elevated in the cerebral spinal fluid (CSF), and detected in meningeal ectopic follicle-like structures as well as active plaques (Krumbholz et al., 2006; Haas et al., 2011; Corcione et al., 2005; Ragheb et al., 2011). Furthermore, the majority of CSF B cells from MS patients are CXCR5⁺ naïve B cells or B_{mem} (Krumbholz et al., 2006; Haas et al., 2011; Cepok et al., 2006; Corcione et al., 2004) supporting a link between elevated intrathecal CXCL13 and the accumulation of class-switched B_{mem} (Haas et al., 2011). CXCL13 and B cells in the CSF are also hallmarks of individuals with Lyme neuroborreliosis (LNB) (Kowarik et al., 2012). In addition, high CXCL13 expression during primary CNS lymphomas, which are predominantly of B cell origin, is associated with inferior outcome as indicated by 10-fold higher CXCL13 levels in the CSF of patients with relapsed primary CNS lymphoma (Rubenstein et al., 2013). While the correlation between CXCL13 and B cell numbers in the CSF in both LNB and

* Corresponding author at: Department of Neurosciences, Lerner Research Institute, The Cleveland Clinic, 9500 Euclid Avenue, NC30, Cleveland, OH 44195, USA.

E-mail addresses: pharest@ccf.org (T.W. Phares), disanok@ccf.org (K.D. DiSano), stohlms2@ccf.org (S.A. Stohlman), bmsegal@med.umich.edu (B.M. Segal), bergmac@ccf.org (C.C. Bergmann).

MS patients (Krumbholz et al., 2006; Kowarik et al., 2012; Rupprecht et al., 2009) supports a causal role for CXCL13 in B cell recruitment to the inflamed CNS, it remains to be formally demonstrated.

Blockade of CXCL13 in animal models of CNS inflammation has yielded mixed results. Mice with chronic-relapsing experimental autoimmune encephalomyelitis (EAE), a model of MS, revealed B cell aggregation proximal to CXCL13 expression in the inflamed meninges (Magliozzi et al., 2004). Moreover, formation of meningeal ectopic follicles and expression of CXCL13 was suppressed by treatment with lymphotoxin- β receptor-Ig fusion protein to disrupt lymphoid organ organization (Columba-Cabezas et al., 2006). By contrast, CXCL13 deficiency did not impair initial B cell recruitment to the CNS in a chronic, non-relapsing EAE model; however, potential effects during peak and chronic disease were not reported as B cell accumulation was only monitored at day 14 post-immunization (Rainey-Barger et al., 2011). B cell accumulation and CXCL13 expression, independent of CNS ectopic follicle-like structures, is also a feature of Sindbis virus infection. However, in this model B cell recruitment to the infected CNS was CXCL13 independent (Rainey-Barger et al., 2011), consistent with only a minor (\sim 1%) fraction of B cells in the CNS expressing CXCR5 (Metcalfe et al., 2013). CNS infection by sublethal glia-tropic JHMV is also associated with CXCL13 upregulation and accumulation of heterogeneous B cell subsets (Phares et al., 2014). ASC accumulation within the CNS is CXCR3-dependent (Marques et al., 2011). Moreover, CXCL13 as a potential mediator of early B cell recruitment is supported by substantially higher expression of CXCR5 transcripts by CNS-infiltrating naïve/early-activated B cells and B_{mem} relative to ASC (Phares et al., 2014). Together these data indicate that local humoral responses within the CNS correlate with but are not necessarily dependent on CXCL13.

The present study sought to define how CXCL13 affects accumulation of distinct B cell subsets during JHMV infection. Following intracranial infection of adult mice JHMV initially replicates in ependymal cells that line the brain ventricles (Wang et al., 1992; Bergmann et al., 2006). Virus then spreads to the parenchyma, where infection is limited to focal areas throughout the brain, but largely sparing the brain stem. Glia are primary targets of infection with sparse neuronal involvement. Early during infection virus replicates prominently in glia and infiltrating macrophages. Once spreading down the central canal of the spinal cord, JHMV moves out into the white matter primarily infecting oligodendrocytes. Virus replication peaks at \sim 5 days post infection (p.i.), and is largely controlled by T cells within 2 weeks p.i. Nevertheless, although infectious virus remains undetectable after 2 weeks, virus persists at low levels as detected by mRNA expression in spinal cords for up to a year (Bergmann et al., 2006; Adami et al., 1995). Importantly, ASC within the CNS are essential to prevent viral reemergence (Ramakrishna et al., 2003; Tschen et al., 2002, 2006).

Infected CXCL13 $^{-/-}$ mice exhibited no deficits in initial accumulation of B cells with a naïve/early phenotype within the CNS. However, the absence of CXCL13 lead to diminished isotype-switched B_{mem} as well as ASC accumulation during persistence, consistent with severely impaired GC B cell and T_{H} cell activation in cervical lymph nodes (CLN). Although ASC expansion in CLN was also negatively affected, there were no evident defects in antiviral serum Ab or ASC recruitment to the bone marrow (BM) in infected CXCL13 $^{-/-}$ relative to wild-type (WT) mice. The results suggest that migration of naïve/early-activated B cells to the CNS is independent of CXCL13 driven signals in the priming lymph nodes or the CNS effector site. Moreover, despite reduced B cell differentiation in the absence of CXCL13, residual humoral immunity is sufficient to establish protective responses in the serum as well as CNS.

2. Materials and methods

2.1. Mice, virus infection and virus titers

C57BL/6 mice were purchased from the National Cancer Institute (Frederick, MD). CXCL13 $^{-/-}$ mice on the C57BL/6 background were previously described (Rainey-Barger et al., 2011) and bred locally. C57BL/6 mice expressing GFP under the glial fibrillary acidic protein (GFAP) promoter were generated by backcrossing FVB/N-Tg (GFAP-GFP) 14Mes/J mice (The Jackson Laboratory, Bar Harbor, ME) onto the C57BL/6 background for at least 10 generations. All mice were housed under pathogen free conditions at an accredited facility at the Cleveland Clinic Lerner Research Institute. Male and female mice were infected indiscriminately at 6–7 weeks of age by intracranial injection with 1000 plaque forming units (PFU) of the J.2.2v-1 monoclonal Ab (mAb)-derived gliotropic JHMV variant (Fleming et al., 1986). Animals were scored daily for clinical signs of disease using the scale: 0, healthy; 1, ruffled fur and hunched back; 2, hind limb paralysis or inability to turn to upright position; 3, complete hind limb paralysis and wasting; 4, moribund or dead. All animal experiments were performed in compliance with guidelines approved by the Cleveland Clinic Lerner Research Institute Institutional Animal Care and Use Committee. Virus titers within the CNS were determined in clarified supernatants by plaque assay using the murine delayed brain tumor (DBT) astrocytoma as detailed (Fleming et al., 1986). Plaques were counted after 48 h incubation at 37 °C.

2.2. Flow cytometry and fluorescence activated cell sorting (FACS)

Pooled brains and spinal cords from 6 to 8 mice perfused with PBS were homogenized in ice-cold Tenbroeck grinders in Dulbecco's PBS. Mononuclear cells were recovered from the 30/70% interface of a Percoll (Pharmacia, Piscataway, NJ) step gradient following centrifugation at 850 \times g for 30 min at 4 °C as detailed (Bergmann et al., 1999). Single-cell suspensions from CLN were prepared as described (Bergmann et al., 1999). For phenotypic analysis pooled cells were stained with mAb specific for CD4 (L3T4), CD8 (53-6.7), CD11b (M1/70), CD19 (1D3), CD25 (PC61), CD45 (30-F11), CD95 (Jo2), CD138 (281-2), GL7 (GL7), IgD (11-26), IgG2 $_{a/b}$ (R2-40) (all from BD Bioscience), IgM (eB121-15F9), PD-1 (RMP1-30) (eBioscience) and F4/80 (CI:A3-1) (Serotec, Raleigh, NC) and analyzed on a BD FACS Aria (BD, Mountain View, CA) using FlowJo 10 software (Tree Star, Ashland, OR). Virus-specific CD8 T cells were identified using D b /S510 major histocompatibility complex (MHC) class I tetramers (Beckman Coulter Inc., Fullerton, CA) as described (Bergmann et al., 1999). CXCR5 surface expression was detected by staining cells with biotin rat anti-mouse CXCR5 Ab (BD Bioscience) and streptavidin phycoerythrin (BD Bioscience).

For RNA expression pooled spinal cords ($n = 6-8$) were digested with collagenase and B cell subsets purified using a BD FACS Aria (BD) as described (Phares et al., 2014). In brief spinal cords were minced and digested in RPMI supplemented with 10% fetal calf serum (FCS), 250 μ l of collagenase D (100 mg/ml) (Roche Diagnostics, Indianapolis, IN) and 50 μ l of DNase I (1 mg/ml) (Roche Diagnostics) for 40 min at 37 °C. Collagenase and DNase I activity was terminated by addition of 0.1 M EDTA (pH 7.2) at 37 °C for 5 min. Following centrifugation, cells were washed with RPMI supplemented with 25 mM HEPES and recovered from the 30/70% interface of a Percoll gradient as described above. Spinal cord CD19 $^{+}$ IgD $^{+}$ B cells at day 7 p.i. were compared to CD19 $^{+}$ CD138 $^{-}$ ASC and CD19 $^{+}$ IgD $^{-}$ B_{mem} from spinal cords purified at day 21 p.i. GFP $^{+}$ CD45 $^{-}$ astrocytes, CD45 lo microglia and CD45 hi CD11b $^{+}$ F4/80 $^{+}$ infiltrating monocyte-derived macrophages were purified from GFAP-GFP pooled spinal cords subsequent to Trypsin digestion as described (Hamo et al., 2007). A minimum of 1×10^5 cells were

collected per pooled sample and frozen in 400 μ l TRIzol (Invitrogen, Carlsbad, CA) at -80°C for subsequent RNA extraction and PCR analysis as described (Phares et al., 2014; Ireland et al., 2009).

2.3. Gene expression analysis

Snap frozen brains, spinal cords or CLN from individual PBS-perfused mice ($n = 3-7$) were placed into Trizol (Invitrogen, Grand Island, NY) and homogenized using a TissueLyser with stainless steel beads (Qiagen, Valencia, CA). RNA was extracted according to the manufacturer's instructions. DNA contamination was removed by treatment with DNase I for 30 min at 37°C (DNA-free kit; Ambion, Austin, TX) and cDNA synthesized using M-MLV Reverse Transcriptase (Invitrogen), oligo-dT primers (20 μ M) (Promega Madison, WI) and random primers (20 μ M) (Promega). Quantitative real-time PCR was performed using 4 μ l of cDNA and SYBR Green Master Mix (Applied Biosystems, Foster City, CA) in duplicate on a 7500 Fast Real-Time PCR System (Applied Biosystems). PCR conditions were 10 min at 95°C followed by 40 cycles at 95°C for 15 s, 60°C for 30 s and 72°C for 30 s. Primers used for transcripts encoding glyceraldehyde 3-phosphate dehydrogenase (GAPDH), a proliferation-inducing ligand (APRIL), CXCL10, CXCL12, IL-10, viral nucleocapsid and IL-21 were previously described (Phares et al., 2009, 2010, 2012; Savarin et al., 2010). GAPDH, CCL19, CCL21, CXCR5, B cell-activating factor of the tumor necrosis factor family (BAFF), gamma interferon (IFN- γ), and activation-induced cytidine deaminase (AID) mRNA levels were determined using Applied Biosystems Gene Expression Arrays with Universal Taqman Fast Master Mix and Taqman primers (Applied Biosystems). PCR conditions were 20 s at 95°C followed by 40 cycles at 95°C for 3 s and 60°C for 30 s. Transcript levels were calculated relative to the housekeeping gene GAPDH using the following formula: $2^{\text{[CT(GAPDH)-CT(Target Gene)]}} \times 1000$, where CT represents the threshold cycle at which the fluorescent signal becomes significantly higher than that of the background.

2.4. ASC enzyme-linked immunospot (ELISPOT) assay

Total and JHMV-specific IgG or IgM ASC were detected by a modification of ELISPOT assay as described (Marques et al., 2011). Briefly spinal cords or brains were minced and digested in 5 ml RPMI supplemented with 10% FCS, 100 μ l of collagenase type I (100 mg/ml; Worthington Biochemical Corporation, Lakewood, NJ) and 50 μ l of DNase I (100 mg/ml) (Roche, Indianapolis, IN) for 40 min at 37°C . Enzyme activity was terminated by addition of 0.1 M EDTA (pH 7.2) at 37°C for 5 min and cells recovered from the 30/70% interface of a Percoll gradient as described above. Single-cell suspensions from CLN or BM were prepared as described (Bergmann et al., 1999). 96-well MultiScreen HTS IP plates (EMD Millipore, Billerica, MA) were coated with either virus ($\sim 5 \times 10^5$ PFU/well) or polyclonal goat anti-mouse Ig (10 μ g/ml; Cappel Laboratories, Inc., Cochranville, PA). Serial dilutions of cells plated in triplicate were incubated for 4 h at 37°C . ASC were detected by sequential incubation with biotinylated rabbit anti-mouse IgG (0.5 μ g/ml; Southern Biotech, Birmingham, AL) or biotinylated goat anti-mouse IgM (1.2 μ g/ml; Jackson ImmunoResearch, West Grove, PA) overnight at 4°C , streptavidin horseradish peroxidase (1:1000; BD biosciences, St. Louis, MO) for 1 h at room temperature, and filtered 3,3'-diaminobenzidine substrate (Sigma-Aldrich, St. Louis, MO) with 30% hydrogen peroxide. Spots were counted using an ImmunoSpot ELISPOT reader (Cellular Technology Ltd., Shaker Heights, OH).

2.5. Histology

CLN from PBS-perfused mice were snap-frozen in Tissue-Tek OCT compound (Sakura Finetex, Torrance, CA) and sectioned at

10 μ m using a Thermo Shandon cryostat. Sections were fixed with ice cold 70% acetone for 5 min, blocked with 5% bovine serum albumin and 10% goat serum for 1 h and then stained with rat anti-mouse FITC conjugated GL7 mAb (BD Biosciences), rat anti-mouse B220 mAb (BD biosciences) and rabbit anti-mouse CD3 polyclonal Ab (Abcam, Cambridge, MA) overnight at 4°C . Samples were then incubated with secondary Ab using Alexa Fluor 594 goat anti-rat (Life Technologies, Grand Island, NY) and Cy5 goat anti-rabbit (Life Technologies, Grand Island, NY) Ab for 1 h at room temperature. Sections were mounted with ProLong Gold antifade reagent with 4',6-diamidino-2-phenylindole (DAPI) (Life Technologies, Grand Island, NY) and examined using a Leica TCS SP5 II fluorescence microscope (Lawrenceville, GA).

2.6. Serum Ab

Virus neutralizing Ab was measured as described (Tschen et al., 2002). Briefly, duplicates of serial 2-fold dilutions of heat inactivated serum from individual mice ($n \geq 5$) were incubated with 50 PFU of JHMV in 96-well plates for 90 min at 37°C . Following addition of DBT cells (8×10^4 cells/well) plates were incubated at 37°C for 48 h. Neutralization titers represent the \log_{10} of the highest average serum dilution that inhibited cytopathic effect. Total virus-specific IgG was measured by ELISA as described (Tschen et al., 2002, 2006). Briefly, plates were coated with 100 μ l of a serum free supernatant derived from JHMV infected DBT cells and incubated overnight at 4°C . Plates were washed with PBS containing 0.05% Tween-20 and blocked with 10% FCS in PBS overnight at 4°C . Serum samples were diluted 2-fold in PBS and incubated overnight at 4°C . Following washing, bound Ab was detected using biotinylated goat anti-mouse IgG (Jackson ImmunoResearch Laboratories), streptavidin horseradish peroxidase (BD Bioscience) and 3,3',5,5' Tetramethylbenzidine (TMB Reagent Set; BD Bioscience). Optical densities were read at 450 nm on a SpectraMax Mz (Molecular Devices, Sunnydale, CA) microplate reader and titers calculated as reciprocals of the highest dilution that exceeded 2-fold \pm standard errors of the means (SEM) over naive controls.

2.7. Collection of CSF and CXCL13 ELISA

CSF was obtained by cisternal puncture performed by a modification of Ronald's method (Li et al., 2006). Following anesthesia, meninges overlying the cisterna magna were exposed and the surrounding area gently washed to prevent blood contamination. A 29-gauge insulin needle was used to puncture the arachnoid membrane covering the cisterna and CSF was collected by gentle pipetting using a polypropylene pipette. Depending on the time-point, about 10–20 μ l of CSF was obtained from each mouse. CSF and clarified brain and spinal cord supernatants were used to measure CXCL13 by ELISA (MCX130; R&D Systems, Minneapolis, MN).

2.8. Statistical analysis

Results are expressed as the means \pm SEM for each group of mice. In all cases, a P value of <0.05 , determined by the unpaired t test, was considered significant. Graphs were plotted and statistics assessed using GraphPad Prism 4.0 software.

3. Results

3.1. Microglia are a primary source of CXCL13 during viral induced neuroinflammation

CXCL13 transcripts are induced and sustained in both brain and spinal cord following JHMV infection (Phares et al., 2014, 2011) in

the absence of apparent ectopic follicle formation. To evaluate if CXCL13 protein is preferentially maintained at distinct anatomical sites after initial clearance of infectious virus at day 14 p.i. CXCL13 was measured in brain, spinal cord and CSF by ELISA (Fig. 1A). CXCL13 was significantly elevated at day 7 p.i. in all three samples (Fig. 1A). While brain CXCL13 declined after day 7 p.i. CXCL13 remained elevated in spinal cord and CSF through day 21 p.i. relative to naïve counterparts (Fig. 1A). To identify the predominant source of CXCL13, astrocytes, microglia and infiltrating monocyte-derived macrophages were purified at day 7 and 10 p.i. and assessed for CXCL13 transcripts. CXCL13 mRNA was predominantly expressed by microglia (Fig. 1B), consistent with other studies (Rainey-Barger et al., 2011; Esen et al., 2014)

3.2. Diminished accumulation of B_{mem} and ASC in absence of CXCL13

Naïve/early-activated B cells accumulate early within the CNS during JHMV infection and are gradually replaced by more differentiated B_{mem} and ASC (Phares et al., 2014), the latter distinguished by expression of the cell surface marker CD138, also known as syndecan-1. While ASC accumulation is CXCR3: CXCL10 dependent (Marques et al., 2011; Phares et al., 2013), chemokines mediating

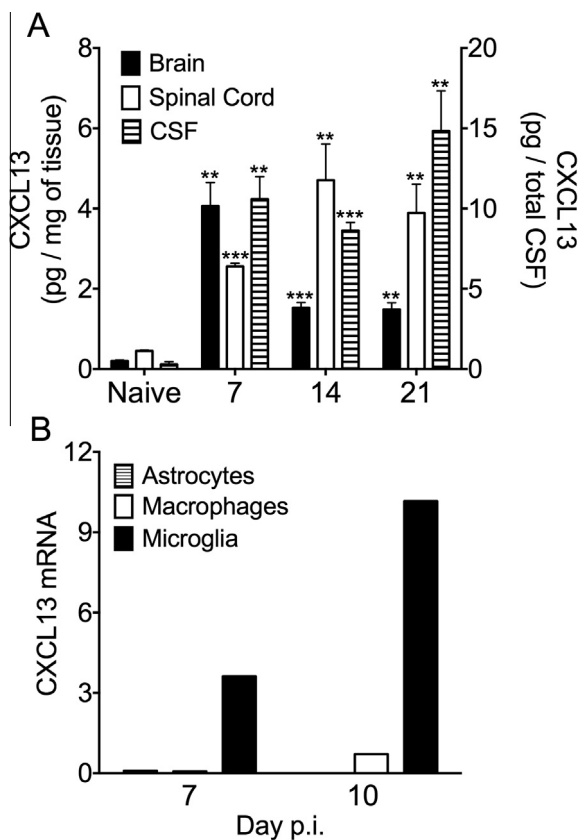


Fig. 1. Microglia are a primary source of CXCL13. (A) Brain, spinal cord and CSF CXCL13 levels from individual mice were assessed by ELISA. Brain and spinal cord data are expressed as the mean CXCL13 per mg of tissue \pm SEM (left-hand y axis) of 6–8 mice per time point from two independent experiments. Typical weights for brain and spinal cord were 397 ± 10 mg and 80 ± 2 mg, respectively. CSF data are expressed as the mean CXCL13 per total CSF volume \pm SEM (right-hand y axis) of 3–4 mice per time point from one experiment. Total volume of mouse CSF is estimated to be 40μ l (Johanson et al., 2008). Significant differences between naïve and infected samples determined by the unpaired t test are denoted by ** ($p < 0.01$) and *** ($p < 0.005$). (B) Relative transcript levels of CXCL13 in FACS-purified GFP⁺CD45⁺ astrocytes (striped bars), CD45^{hi}CD11b⁺F4/80⁺ monocyte-derived macrophages (empty bar) or CD45^{lo} microglia (solid bar) derived from pooled spinal cords of 6–8 GFAP-GFP mice per time point collected at 7 and 10 days p.i. were assessed by real-time PCR. Transcript levels are relative to GAPDH.

CNS recruitment of other B cell subsets are unknown. CXCL13 dependent accumulation of naïve/early-activated B cells (CD138⁻ IgD⁺ IgM⁺) and B_{mem} (CD138⁻ IgD⁻ IgM⁺) is supported by higher CXCR5 transcript expression in both populations relative to CNS-derived CD138⁺ ASC (Fig. 2A). CNS accumulation of naïve/early-activated B cells, B_{mem} , as well as ASC in infected WT and CXCL13^{-/-} mice was thus assessed by flow cytometry (Fig. 2B–E). Fig. 2B shows a representative plot defining CD138⁻ IgD⁺ IgM⁺ naïve/early-activated B cells and CD138⁻ IgD⁻ IgM⁺ B_{mem} . Although analysis focused on the spinal cord as the target of viral persistence and sustained CXCL13 levels, results were overall similar in the brain (data not shown). Total CD19⁺ B cell numbers were independent of CXCL13, regardless of the day p.i. (data not shown). The number of naïve/early-activated B cells, comprising the vast majority of B cells at day 7 p.i. but declining thereafter (Phares et al., 2014), were also comparable between WT and CXCL13^{-/-} mice throughout infection (Fig. 2C). B_{mem} numbers were similar at day 7 p.i. in both groups; however, while they nearly doubled in WT mice between day 7 and day 14 p.i. B_{mem} did not increase in the absence of CXCL13 (Fig. 2D). By day 21 p.i. B_{mem} numbers were comparable in both groups due to their decline in WT mice. Initial CD138⁺ ASC accumulation at day 14 p.i. was similar and increased by day 21 p.i. in both groups, but only reached ~50% of the levels in WT mice in absence of CXCL13 (Fig. 2E). Furthermore, the number of CD138⁺ ASC still remained lower in infected CXCL13^{-/-} versus WT mice at day 42 p.i. (CXCL13^{-/-} = 195 versus WT = 425). ELISPOT analysis of brain- and spinal cord-derived ASC was performed at day 21 p.i. to reveal whether impaired accumulation was restricted to virus-specific ASC and/or a specific Ig isotype. The number of total and virus-specific IgM⁺ ASC were similar in the CNS of WT and CXCL13^{-/-} mice (Fig. 3A and B). However, the absence of CXCL13 resulted in 2- to 3-fold lower total and virus-specific IgG⁺ ASC in brains and spinal cords, respectively (Fig. 3C and D). These data argue that CXCL13 is dispensable for early accumulation of naïve/early-activated B cell in the CNS, but promotes both B_{mem} and specifically IgG⁺ ASC accumulation as the naïve/early-activated B cell population declines.

3.3. CXCL13 deficiency impairs peripheral GC formation

Generation of T dependent isotype-switched ASC and B_{mem} following infections or immunizations is driven by antigen-specific B cell and CD4⁺ T_H engagement within GC (Victora and Nussenzweig, 2012; Zotos and Tarlinton, 2012). CXCR5 expressed on both activated B and CD4⁺ T_H cells promotes antigen-specific B cell expansion and enhances GC formation especially under conditions of limiting antigen load (Junt et al., 2005). Reduced IgG⁺ ASC accumulation in the CNS of JHMV infected CXCL13^{-/-} mice thus suggested a defect in peripheral expansion due to impaired GC formation. Following JHMV infection both T and B cell activation occurs primarily in CLN. Although CXCL13^{-/-} and CXCR5^{-/-} mice have developmental defects in the formation of most lymph nodes (Ansel et al., 2000; Forster et al., 1996), CLN and mesenteric LN are not disrupted in CXCL13^{-/-} mice (Ansel et al., 2000). This was confirmed by similar CLN cellularity in naïve WT and CXCL13^{-/-} mice (data not shown). B cell activation in the draining CLN following infection was therefore monitored for GL7⁺ CD95⁺ B cells by flow cytometry. GL7, also known as T and B cell activation marker and CD95, also known as FAS receptor are phenotypic markers of activated GC B cells (van Eijk et al., 2001; Cervenak et al., 2001). Frequencies of GC-derived B cells (CD19⁺ GL7⁺ CD95⁺) were already increased at day 7 p.i. in both infected WT and CXCL13^{-/-} mice relative to naïve controls (Fig. 4A). However, whereas GC B cells increased and remained elevated through day 21 p.i. in WT mice, they failed to increase in CXCL13^{-/-} mice (Fig. 4A). Impaired GC formation was supported by significantly

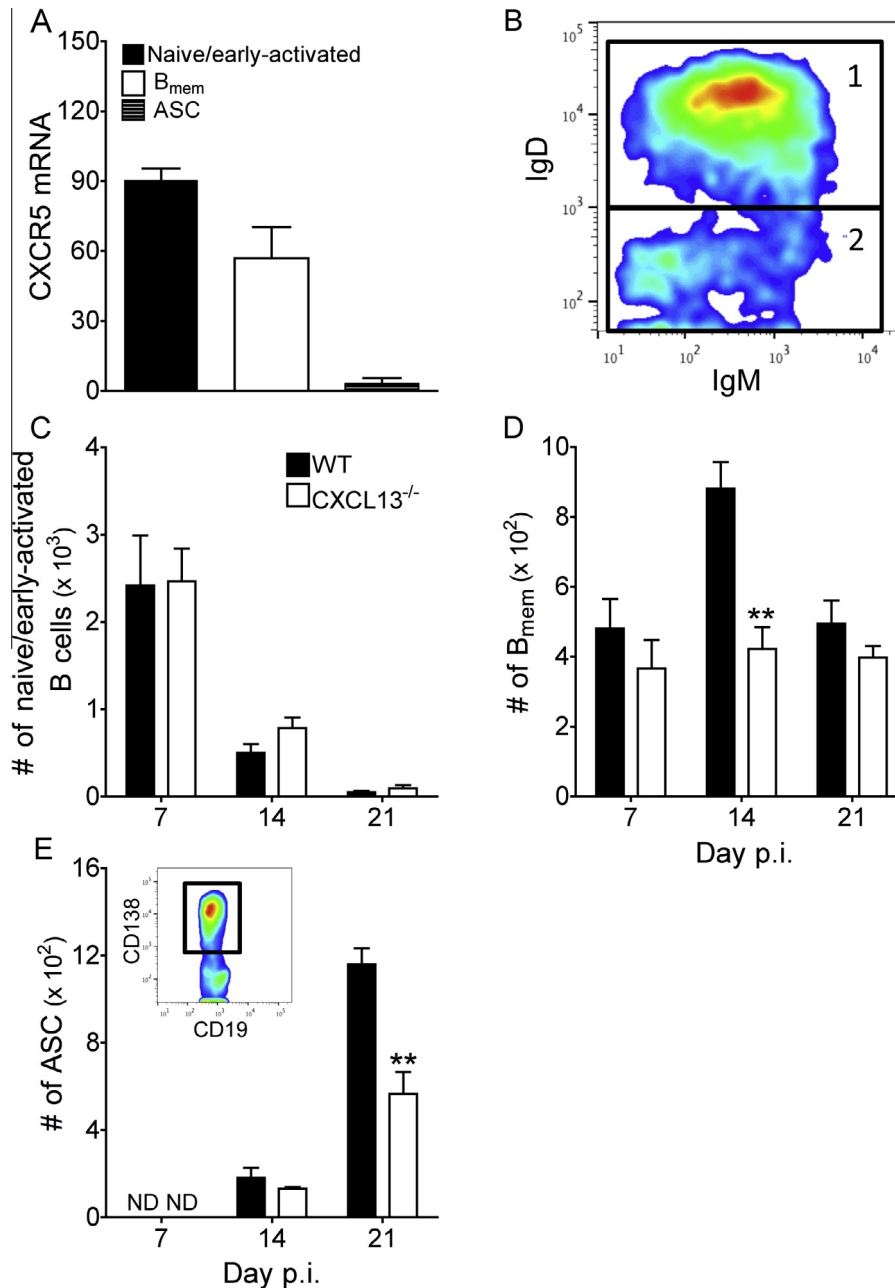


Fig. 2. Reduced CNS accumulation of B_{mem} and ASC in the absence of CXCL13. (A) Relative transcript levels of CXCR5 assessed by real-time PCR in naive/early-activated B cells ($CD138^+IgD^+$), B_{mem} ($CD138^+IgD^-$) and ASC ($CD138^+$) FACS-purified from pooled spinal cords of 6–8 mice per time point collected at 7 (naive/early-activated B cells) or 21 (B_{mem} and ASC) days p.i. Data are expressed as the mean \pm SEM transcript level relative to GAPDH mRNA and represent two independent experiments. (B) Representative density plot of IgD and IgM expression on spinal cord-derived $CD19^+CD138^-$ B cells at day 14 p.i. Gated populations are as follows: 1 = naive/early-activated B cells IgD^+IgM^+ ; 2 = B_{mem} $IgD^-IgM^{+/-}$. (C and D) Numbers of IgD^+IgM^+ and $IgD^-IgM^{+/-}$ B cells within total $CD19^+CD138^-$ B cells. (E) Numbers of $CD138^+$ ASC within $CD19^+$ B cells. Insert: Representative density plot of CD138 expression (gated cells) on spinal cord-derived $CD19^+$ B cells at day 21 p.i. Data are expressed as the mean \pm SEM and represent three independent experiments, each comprising pooled spinal cords of 3–4 mice per time point. ND = not detected. Significant differences between WT and $CXCL13^{-/-}$ mice determined by the unpaired t test are denoted by ** ($p < 0.01$).

reduced upregulation of transcript levels encoding AID, an enzyme upregulated in activated GC-derived B cells (Keim et al., 2013; Maul and Gearhart, 2010; Muramatsu et al., 2000), in CLN of $CXCL13^{-/-}$ relative to WT mice (Fig. 4B). By contrast, transcripts for CXCL12, CCL19, and CCL21, chemokines regulating B cell migration within lymph node follicles (Cyster, 2005; Okada and Cyster, 2006), were not impaired by CXCL13 deficiency (Fig. 4C). CXCL12 mRNA levels remained at similar and constant levels throughout infection, while CCL19 and CCL21 mRNA levels were even significantly elevated after day 7 p.i. in the absence of CXCL13 (Fig. 4C),

potentially altering trafficking of $CCR7^+$ lymphocytes or dendritic cells (Craft, 2012; Scandella et al., 2007). In contrast to GC-phenotype B cells, expansion of early short-lived $CD138^+$ ASC prior to day 10 p.i. was CXCL13 independent (data not shown).

To assess whether impaired B cell activation in CLN coincided with reduced T cell help, T_H cells ($CD4^+CXCR5^+PD-1^{\text{hi}}$) were compared between the groups. T_H frequencies were significantly increased relative to naive levels by day 7 p.i. in both WT and $CXCL13^{-/-}$ mice and remained elevated through day 21 p.i. (Fig. 4D). However, percentages were consistently lower in the

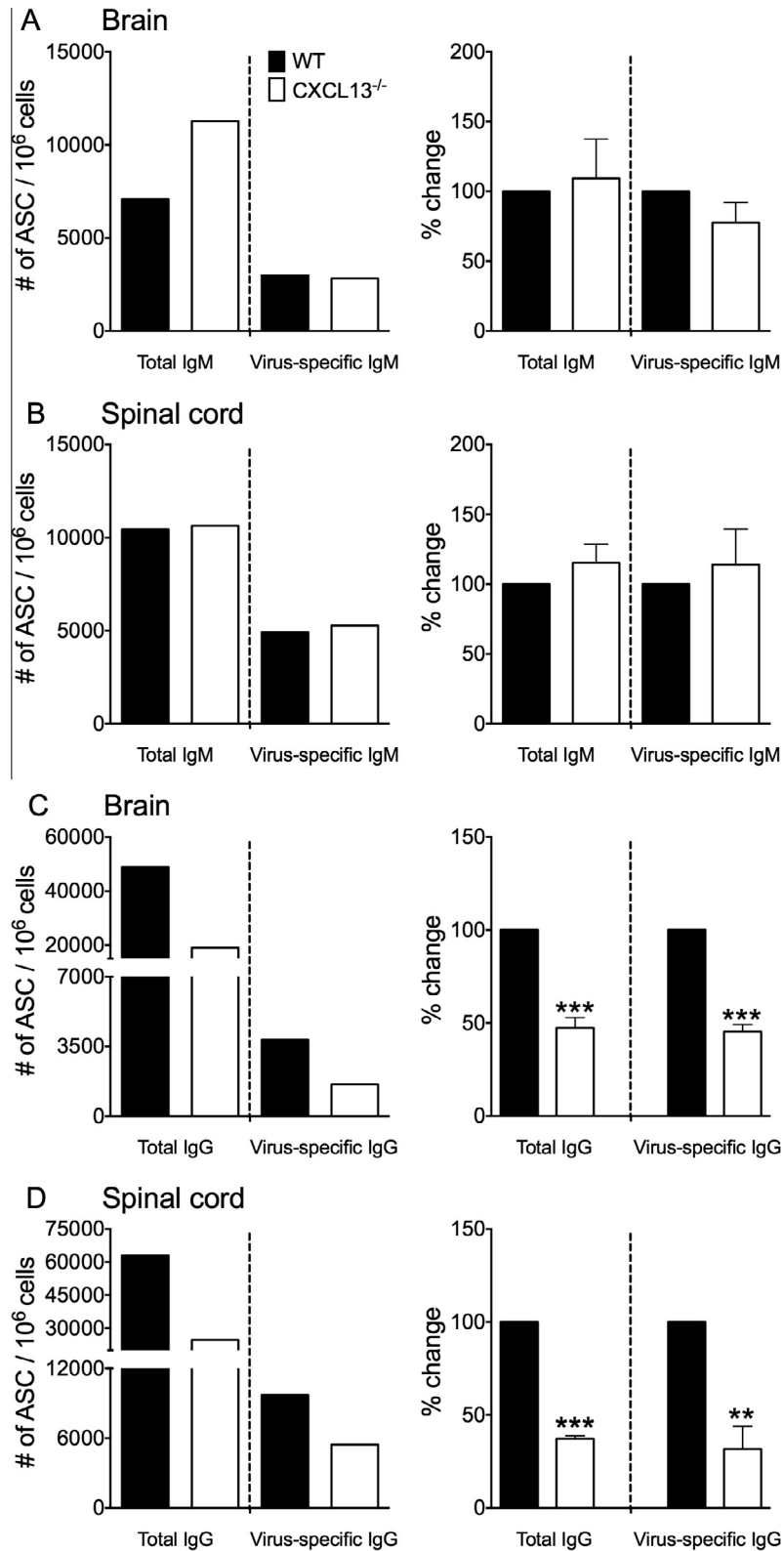


Fig. 3. Reduced CNS accumulation of virus-specific IgG⁺ ASC in CXCL13^{-/-} mice. Numbers of total and virus-specific IgM (A and B) or IgG-secreting (C and D) ASC in brain (A and C) or spinal cord (B and D) measured by ELISPOT assay (left column). Data are representative of 2–3 independent experiments with similar trends in each experiment. To better reflect relative differences between WT and CXCL13^{-/-} frequencies, data in the right column show the mean percentage changes in frequencies \pm SEM calculated relative to levels in WT mice, which were set to a baseline value of 100. Data represent 2–3 independent experiments, each comprising pooled brain or spinal cords of 3–4 mice. Significant differences between WT and CXCL13^{-/-} mice determined by the unpaired *t* test are denoted by ** ($p < 0.01$) and *** ($p < 0.005$).

absence of CXCL13 (Fig. 4D). IL-21 is a T_H17-derived cytokine that promotes GC reactions and generation of ASC (Zotos et al., 2010; Ozaki et al., 2002; Rankin et al., 2011; Linterman et al., 2010).

Decreased expression of IL-21 transcripts in CLN mRNA from CXCL13^{-/-} mice supported impaired T_H17 activity (Fig. 4E). Of note, similar CLN frequencies of virus-specific CD8⁺ T cells and

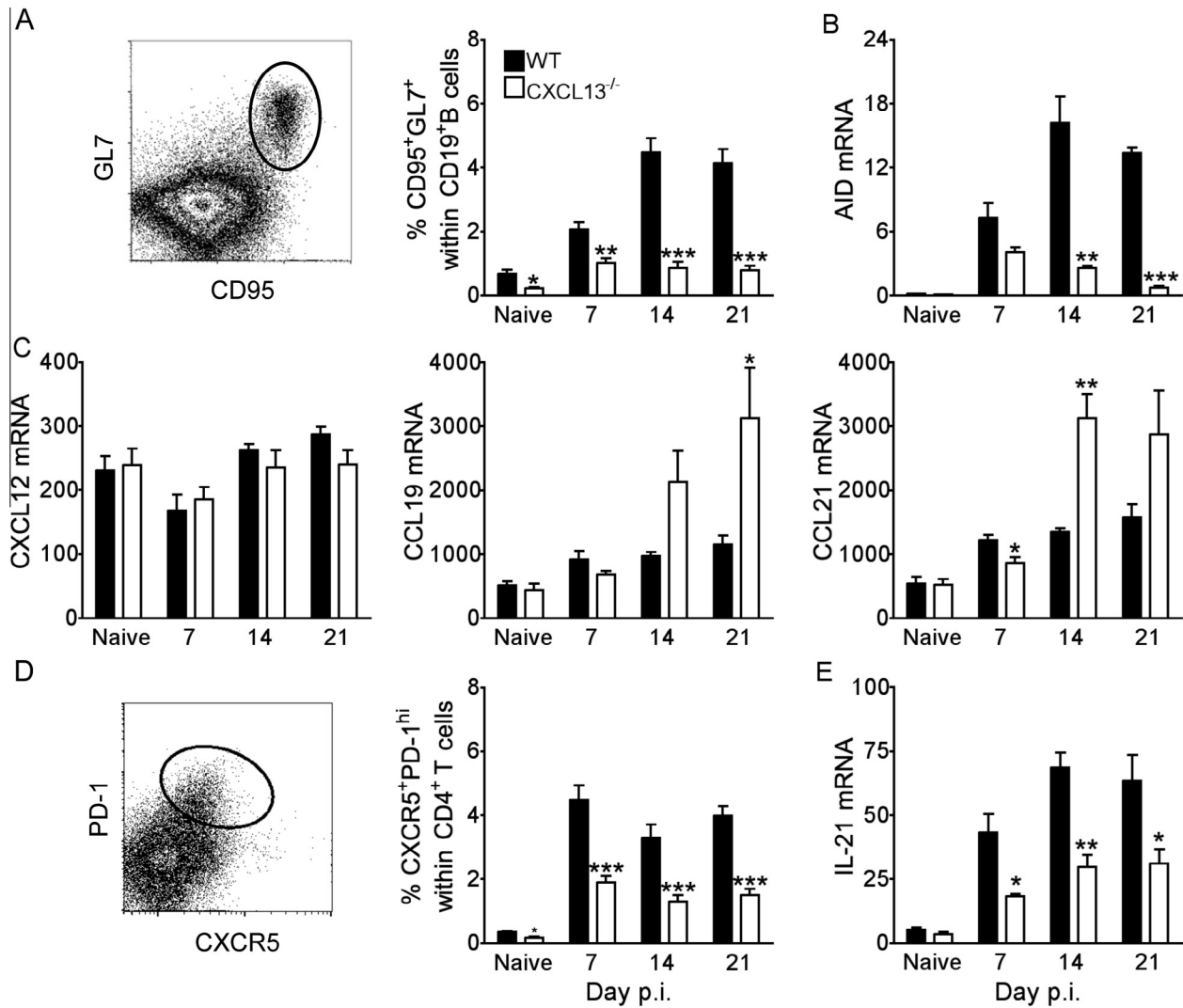


Fig. 4. Impaired activation of GC B cells and T_H cells in CLN of CXCL13^{-/-} mice. (A) Representative density plot of CD95 and GL7 expression on WT CLN-derived CD19⁺ B cells at day 14 p.i. Frequencies of CD95⁺GL7⁺ cells with total CD19⁺ B cells determined by flow cytometry. Data are expressed as the mean percentage \pm SEM of 6–8 mice per time point from two independent experiments. Relative transcript levels of AID (B), CXCL12, CCL19 and CCL21 (C) in CLN of naive and infected mice assessed by real-time PCR. (D) Representative density plot of CXCR5 and PD-1 expression on WT CLN-derived CD4⁺ T cells at day 14 p.i. The proportion of CXCR5⁺PD-1^{hi} cells within total CD4⁺ T cells determined by flow cytometry. Data are expressed as the mean percentage \pm SEM of 6–8 mice per time point from two independent experiments. (E) Relative transcript levels of IL-21 in CLN of naive and infected mice assessed by real-time PCR. All PCR data are expressed as the mean transcript level \pm SEM relative to GAPDH mRNA and represent one experiment comprising individual CLN of 3 to 4 mice per time point. Significant differences between WT and CXCL13^{-/-} mice determined by the unpaired *t* test are denoted by * ($p < 0.05$), ** ($p < 0.01$) and *** ($p < 0.005$).

CD4⁺CD25⁺ T cells in WT and CXCL13^{-/-} mice (data not shown) imply CXCL13 deficiency specifically affects T_H cells. To confirm impaired GC B cell and T_H cell activation in CXCL13^{-/-} mice coincides with poor GC development CLN were screened for discrete areas of T cell (CD3⁺) and B cell (B220⁺GL7⁺) co-localization as readout for GC formation. While GC were readily detected by day 14 p.i. (data not shown) and continued to mature through day 21 p.i. in WT mice, both the number and size of GC were noticeably smaller in CXCL13^{-/-} mice (Fig. 5). Impaired GC formation thus suggested reduced peripheral humoral responses are responsible for decreased CNS accumulation of IgG⁺ ASC. Surprisingly however, no differences in either virus-specific IgG or neutralizing Ab were detected in serum between WT and CXCL13^{-/-} mice (Fig. 6A). To assess whether ASC matured independent of GC, virus-specific ASC were monitored in CLN and BM, the preferential site for long-term retention of protective ASC (Cyster, 2003). The frequency of virus-specific IgG ASC in CLN were only marginally reduced in the absence of CXCL13 at day 21 p.i., despite limited GC formation (Fig. 6B). Furthermore, IgG⁺ ASC frequencies in BM

were similar or slightly higher in CXCL13^{-/-} relative to WT mice (Fig. 6C), consistent with intact serum Ab. Taken together the data indicate that CXCL13-dependent organized GC are not essential for mounting effective serum Ab responses following CNS infection. Moreover, although slightly impaired peripheral expansion coincided with reduced ASC accumulation in the CNS of CXCL13^{-/-} mice, ASC in BM were intact. These results suggested CXCR4 driven ASC recruitment to BM is not affected by CXCL13 deficiency, whereas reduced activation in CLN limits CXCR3 dependent accumulation to the inflamed CNS.

3.4. Impaired ASC accumulation in CXCL13^{-/-} mice is sufficient to control persisting virus

CNS-localized ASC are crucial in preventing viral recrudescence of persisting JHMV (Ramakrishna et al., 2003; Tschen et al., 2002, 2006). To assess whether diminished ASC accumulation in the CNS of CXCL13^{-/-} mice altered JHMV pathogenesis, viral control was examined by monitoring infectious virus and transcripts

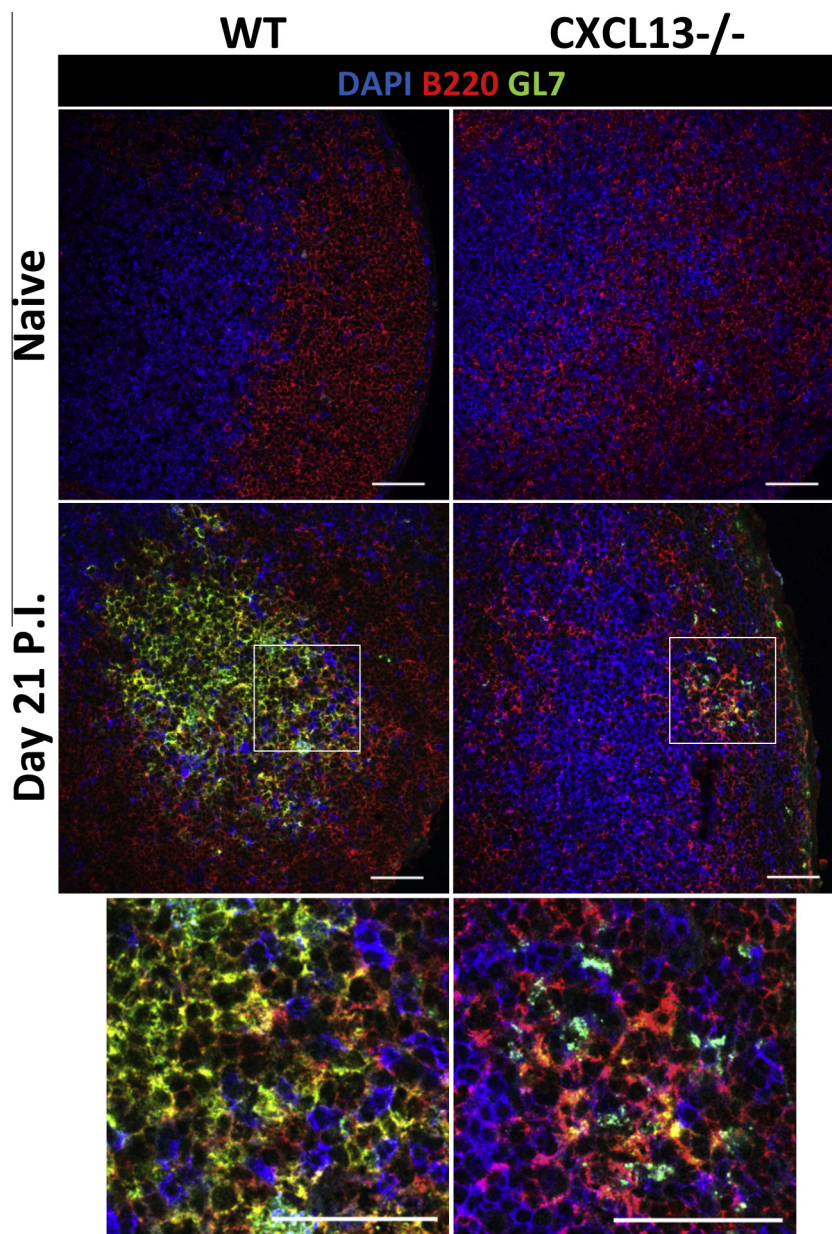


Fig. 5. GC formation is severely abrogated in CXCL13^{-/-} mice. GC formation in the CLN of WT and CXCL13^{-/-} mice at day 21 p.i. analyzed using DAPI (blue), anti-GL7 (green) and anti-B220 (red) Ab. GL7⁺ B cells are absent or sparse in naïve WT and CXCL13^{-/-} mice respectively. Merged images are shown. Photomicrographs are presented at a magnification of 40 \times . Scale bar is 50 μ m. White-boxed area shown in bottom row photomicrographs. (For interpretation of the references to color in this figure legend, the reader is referred to the web version of this article.)

encoding the viral nucleocapsid protein. Overall onset, progression and peak of clinical disease were comparable in WT and CXCL13^{-/-} mice (Fig. 7A). Infectious virus was similar in both groups at day 5 and controlled with similar kinetics by day 14 p.i. (Fig. 7B). By day 21 p.i. infectious virus was below detection in both groups with the exception of a single CXCL13^{-/-} mouse. Importantly, infectious virus remained undetectable through day 42 p.i. (Fig. 7B). Similarly low persisting viral transcripts in the spinal cord of both groups further demonstrated ongoing viral control (Fig. 7C). No alterations in antiviral T cell-mediated immunity in the absence of CXCL13 was supported by comparable spinal cord-derived transcripts for T cell-derived cytokines including IFN- γ , IL-10 and IL-21 between WT and CXCL13^{-/-} mice (Fig. 7D–F). Notably, there were also no differences in CXCL9 or CXCL10 mRNA levels, suggesting signals for CXCR3 dependent ASC recruitment were not impaired (data not shown). Expression of transcripts encoding chemokines

CXCL12, CCL19 and CCL21, potentially affecting recruitment of CXCR4 or CCR7 expressing B cells were also intact in CXCL13^{-/-} mice (Fig. 7G–I). Although CCL21 mRNA was not induced by infection in either group, CCL21 transcripts were 10-fold higher at basal levels and throughout infection in CXCL13^{-/-} relative to WT mice (Fig. 7I). Notably, cytokine and chemokine expression profiles were similar in the brain (data not shown). These results indicate that control of persistence by the CNS humoral response is independent of CXCL13 despite the diminished number of isotype-switched virus-specific ASC.

4. Discussion

CXCL13 is upregulated in the CNS during various microbial infections as well as autoimmune inflammation, yet its role in

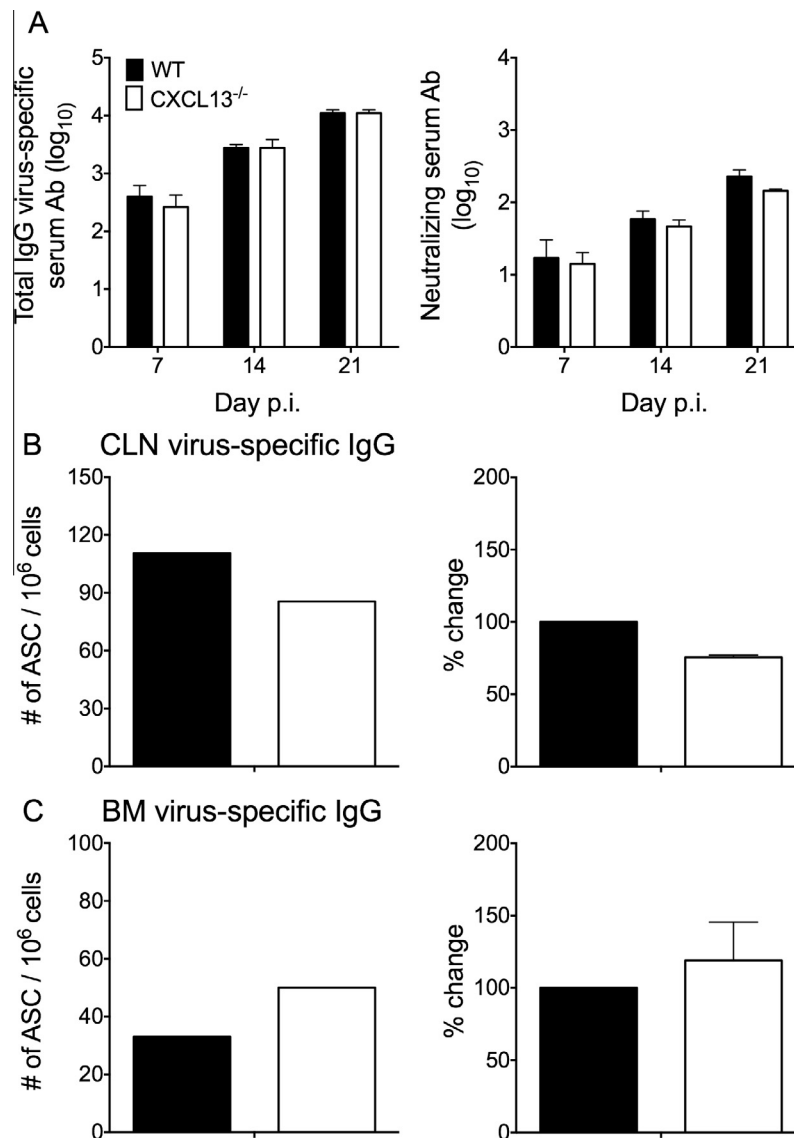


Fig. 6. Peripheral ASC responses are intact in CXCL13^{-/-} mice. (A) Virus-specific IgG2a and neutralizing Ab in serum of infected WT and CXCL13^{-/-} mice. Data are expressed as the mean \pm SEM and represent two independent experiments, each comprising individual sera of 3 mice per time point. Numbers of virus-specific IgG-secreting ASC in CLN (B) and BM (C) measured by ELISPOT assay. Data are representative of 2–3 independent experiments with similar trends in each experiment. To better reflect relative differences between WT and CXCL13^{-/-} frequencies, data in the right column of (B and C) show the mean percentage changes in frequencies \pm SEM calculated relative to levels in WT mice, which were set to a baseline value of 100. Data represent 2–3 independent experiments, each comprising pooled CLN or BM from 3 to 4 mice.

CNS humoral immunity remains unclear (Finch et al., 2013; Krumbholz et al., 2006; Rupprecht et al., 2009; Rainey-Barger et al., 2011; Metcalf et al., 2013; Phares et al., 2014; Gelderblom et al., 2007; Khademi et al., 2011). The data herein demonstrate that CXCL13 induced by gliatropic JHMV infection remains elevated in CSF at least a week post clearance of infectious virus; however, it is not essential in recruiting naïve/early-activated IgD⁺ B cells into the CNS, although this population expresses high levels of CXCR5 mRNA. CXCL13 deficiency affected B_{mem} accumulation transiently, but the major impact was on CD138⁺ ASC previously shown to require CXCR3: CXCL10 to migrate into the CNS (Marques et al., 2011). CNS-derived ASC were reduced by 50%, specifically affecting isotype-switched IgG⁺, but not IgM⁺ ASC.

Unaltered accumulation of IgD⁺ naïve/early-activated B cells within the CXCL13^{-/-} CNS implies chemokine receptors other than CXCR5 mediate their trafficking. Similar CCR7 and higher CXCR4 transcript expression by CNS-derived IgD⁺ naïve/early-activated B cells relative to CLN-derived IgD⁺ B cells (Phares et al., 2014) implicate CXCR4 and/or CCR7 in driving recruitment. Notably, elevated

CCL19 transcripts in the CNS during JHMV infection (Phares et al., 2014) are consistent with preferential recruitment of IgD⁺ naïve/early-activated B cells via CCR7. CXCL13 independent recruitment of early B cells was also noted following both Sindbis virus infection and induction of EAE (Rainey-Barger et al., 2011), supporting the notion that CXCL13 is not an effective target to manipulate B cell recruitment early during CNS inflammation. Moreover, during Sindbis virus infection CCL19 transcripts are elevated early in the CNS coinciding with peak numbers of CCR7⁺ B cells (Metcalf et al., 2013).

The primary effect of CXCL13 deficiency on CNS accumulation of isotype-switched B cells correlated with reduced activation of GL7⁺ GC-derived B cells as a result of impaired CLN GC formation. CXCL13 recruits activated CXCR5⁺ T_H cells into the GC where IL-21, the signature T_H cytokine, promotes ASC and B_{mem} differentiation (Ozaki et al., 2002; Rankin et al., 2011; Linterman et al., 2010; Rasheed et al., 2013). Impaired T_H activation, coincident with reduced IL-21 mRNA in CXCL13^{-/-} CLN, implied that reduced isotype-switched B cell accumulation in the CNS was

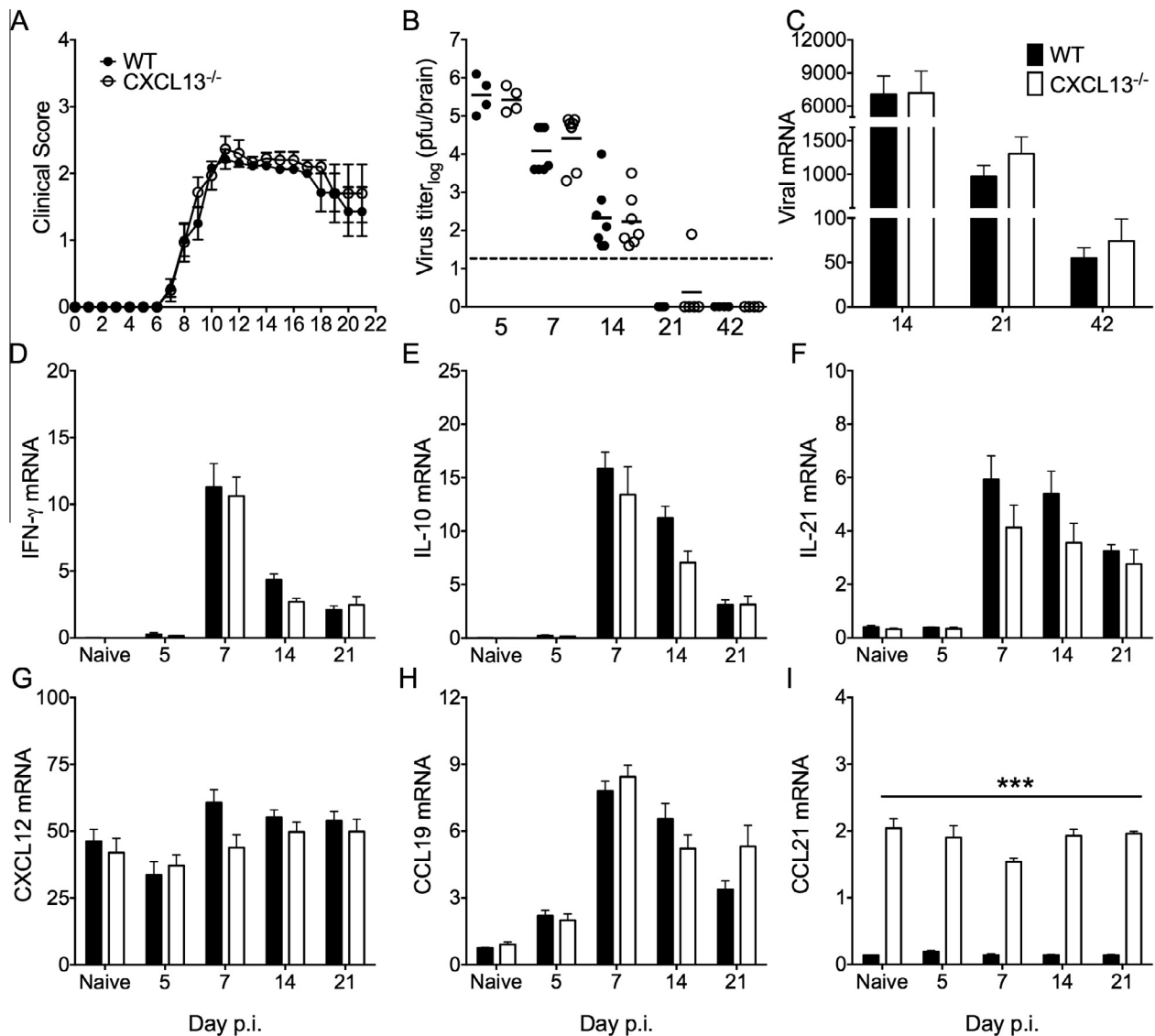


Fig. 7. CXCL13 deficiency does not affect JHMV pathogenesis or viral control. (A) WT and CXCL13^{-/-} infected mice were monitored daily for clinical symptoms. (B) Virus titers in brain supernatants determined by plaque assay and expressed as the mean \pm SEM. Dashed line marks the limit of detection. Data are on a log₁₀ scale. Relative transcript levels of viral nucleocapsid (C), IFN- γ (D), IL-10 (E), IL-21 (F), CXCL12 (G), CCL19 (H) and CCL21 (I) in spinal cords of naïve and infected mice assessed by real-time PCR. All PCR data are expressed as the mean transcript level \pm SEM relative to GAPDH mRNA of 6–7 mice per time point from two independent experiments. Significant differences between WT and CXCL13^{-/-} mice determined by the unpaired *t* test are denoted by *** (*p* < 0.005).

predominantly attributed to deficient peripheral B cell differentiation rather than local CNS defects. Indeed, CNS-derived IL-21 transcripts, expressed primarily by CD4⁺ T cells during JHMV infection (Phares et al., 2013), were not altered by CXCL13 deficiency. Thus, although inflamed sites expressing CXCL13 may recruit circulating CXCR5⁺ T_H cells and thereby promote local B cell differentiation, CXCL13 independent IL-21 mRNA levels in the CNS argue against a local role of T_H cells in gliotropic JHMV infection. Furthermore, preliminary analysis shows no evidence for a CXCR5⁺ T_H phenotype in the CNS of JHMV-infected mice. Hence although CXCL13 driven CXCR5⁺ T cells are implicated in prolonging pathology during EAE (Bagaeva et al., 2006), our data suggest IL-21 expressing CD4 T cells in the JHMV-infected CNS are not regulated by CXCL13 and may comprise a distinct effector CD4 T cell subset. In this context it is of interest to note that IL-21 can be secreted by multiple CD4 T cell subsets (Yi et al., 2010).

Given the defect in GC formation, it was surprising that virus-specific IgG serum Ab, including neutralizing Ab, production was not impaired in absence of CXCL13. Similar results following CNS

Sindbis virus infection (Rainey-Barger et al., 2011) imply that well organized follicles with clearly defined GC structures are not essential for effective peripheral antiviral humoral responses. Although GC formation was impaired in JHMV-infected CXCL13^{-/-} CLN, there was evidence for focal clustering of B and T cells at the time of GC formation in WT mice. Such focal sites of T and B cell aggregation may be supported by elevated expression of the CCR7 ligands CCL19 and CCL21 at days 14 and 21 p.i. in CXCL13^{-/-} relative to WT mice. CCR7 is increased on antigen engaged WT B cells, directing early-activated B cells to migrate to the T cell zone chemokines CCL19 and CCL21 (Reif et al., 2002). During peripheral Vesicular Stomatitis virus infection CCR7 plays a critical role in driving B:T helper cell collaboration at the T:B cell border (Scandella et al., 2007). Similarly, CCR7 enhanced interactions of antigen primed B cells and T helper cells may facilitate B cell differentiation during JHMV infection in absence of CXCL13. This is supported by only slightly reduced numbers of virus-specific IgG⁺ ASC in CLN and no ASC defects in BM of CXCL13^{-/-} relative to WT mice.

Regulation and function of chemokine receptors on B cell subsets has been prominently described for events involving inter-compartmental migration within lymphoid tissue, but not to sites of infection. In addition to distinct expression and regulation of various receptors on CNS-derived activated IgD⁺ B cells versus B_{mem} in infected WT mice (Phares et al., 2014), impaired GC formation in absence of CXCL13 may further skew signaling by other chemokines acting via CXCR4 or CCR7. The extensive downregulation of both CXCR5 and CXCR4, but to a lesser extent CCR7, on CNS-derived WT B_{mem} versus activated IgD⁺ B cells (Phares et al., 2014) suggests B_{mem} are recruited by CXCR5: CXCL13 independent mechanisms and should thus not be affected by CXCL13 deficiency. However, it cannot be excluded that impaired GC formation alters imprinting of signals required for early B_{mem} egress from lymphoid tissue into the circulation, thereby explaining the difference to WT mice at day 14 p.i. Distinguishing between CXCL13 dependent B_{mem} egress into circulation, migration or survival in the CNS will be pursued in future studies.

CXCL13 as well as CXCR5 independent peripheral isotype-switched B cell responses have been noted in other experimental models (Rainey-Barger et al., 2011; Junt et al., 2005). However, comparative analysis of distinct peripheral infections and protein immunization demonstrated that CXCR5 is particularly critical to augment humoral responses under conditions of low antigenic load (Junt et al., 2005). The overall efficient CXCL13 independent, albeit CD4 T cell dependent (Phares et al., 2012), virus-specific ASC responses following JHMV infection were thus surprising given poor peripheral replication of JHMV following intracranial infection. However, the present data do not exclude the possibility of protective extrafollicular responses in absence of CXCL13, especially if CD4 T cell help can be provided despite perturbed follicular structure. B cell activation and GC formation following JHMV infection is limited to the draining CLN, with little ASC expansion noted in the spleen (Marques et al., 2011). To what extent either cell free or dendritic cell-associated viral antigen drainage gives rise to effective humoral immunity remains to be resolved. Nevertheless, our results demonstrate that GC formation is CXCL13 driven; however, CLN GC reactions are not essential to initiate isotype-switching under conditions of low viral load. Furthermore, similar frequencies of IgG⁺ virus-specific ASC in BM of CXCL13^{-/-} and WT mice suggest CXCR4 driven migration to BM is independent of imprinting in fully formed GC. Interestingly however, reduced accumulation of ASC in the CXCL13^{-/-} CNS suggests less efficient CXCR3 driven migration to inflamed sites. In WT mice, CXCR3 expression on CLN-derived ASC is increased between day 7 and 14 p.i. (Marques et al., 2011), coincident with initiation of GC formation. Altered chemokine receptor regulation on virus-specific IgG⁺ ASC in absence of CXCL13 may thus lead to preferential default migration to BM. Additionally, less organized B cell structures may impose distinct patterns of migration within lymph nodes, thereby affecting CLN egress into the circulation.

In conclusion, our results demonstrate that early CNS accumulation of IgD⁺ B cells is independent of CXCL13. Furthermore, CXCL13: CXCR5 independent B:T helper cell interactions, likely driven by CCR7-mediated migration, are sufficient to elicit isotype-switched, virus-specific IgG⁺ ASC and neutralizing serum Ab in the periphery, despite significantly impaired GC formation. These data suggest CXCL13 may not be a driving force in the seeding of B cell aggregates or follicle-like structures in non-lymphoid organs, which are thought to aggravate local autoimmunity (Finch et al., 2013; Parker Harp et al., 2015). Importantly, GC independent differentiation of antigen-specific B cells in lymphoid tissue implies similar events may occur at inflammatory sites characterized by elevated CCR7 ligand expression to promote B:T helper cell interactions. Expression of various cytokines and chemokines sustain-

ing humoral immunity in the inflamed CNS may thus suffice to maintain local humoral responses independent of CXCL13.

Acknowledgments

This work was supported by U.S. National Institutes of Health Grant NS064932 (C.C.B) and a 2015 U.S. National Institutes of Health shared instrument award to the Lerner Research Institute Imaging Core for the Leica TCS-SP5II. The funding source had no involvement in study design, writing of the manuscript, decision to submit or collection, analysis and interpretation of data. We sincerely thank Natasha Towne and Mi Widness for gene expression analysis.

References

- Adami, C., Pooley, J., Glomb, J., Stecker, E., Fazal, F., Fleming, J.O., Baker, S.C., 1995. Evolution of mouse hepatitis virus (MHV) during chronic infection: quasispecies nature of the persisting MHV RNA. *Virology* 209, 337–346.
- Ansel, K.M., Ngo, V.N., Hyman, P.L., Luther, S.A., Forster, R., Sedgwick, J.D., Browning, J.L., Lipp, M., Cyster, J.G., 2000. A chemokine-driven positive feedback loop organizes lymphoid follicles. *Nature* 406, 309–314.
- Bagaeva, L.V., Rao, P., Powers, J.M., Segal, B.M., 2006. CXCL chemokine ligand 13 plays a role in experimental autoimmune encephalomyelitis. *J. Immunol.* 176, 7676–7685.
- Bergmann, C.C., Altman, J.D., Hinton, D., Stohlman, S.A., 1999. Inverted immunodominance and impaired cytolytic function of CD8⁺ T cells during viral persistence in the central nervous system. *J. Immunol.* 163, 3379–3387.
- Bergmann, C.C., Lane, T.E., Stohlman, S.A., 2006. Coronavirus infection of the central nervous system: host-virus stand-off. *Nat. Rev. Microbiol.* 4, 121–132.
- Cepok, S., von Geldern, G., Grummel, V., Hochgesand, S., Celik, H., Hartung, H., Hemmer, B., 2006. Accumulation of class switched IgD-IgM- memory B cells in the cerebrospinal fluid during neuroinflammation. *J. Neuroimmunol.* 180, 33–39.
- Cervenak, L., Magyar, A., Boja, R., Laszlo, G., 2001. Differential expression of GL7 activation antigen on bone marrow B cell subpopulations and peripheral B cells. *Immunol. Lett.* 78, 89–96.
- Columba-Cabezas, S., Griguoli, M., Rosicarelli, B., Magliozzi, R., Ria, F., Serafini, B., Aloisi, F., 2006. Suppression of established experimental autoimmune encephalomyelitis and formation of meningeal lymphoid follicles by lymphotoxin beta receptor-Ig fusion protein. *J. Neuroimmunol.* 179, 76–86.
- Corcione, A., Casazza, S., Ferretti, E., Giunti, D., Zappia, E., Pistorio, A., Gambini, C., Mancardi, G.L., Uccelli, A., Pistoia, V., 2004. Recapitulation of B cell differentiation in the central nervous system of patients with multiple sclerosis. *Proc. Natl. Acad. Sci. USA* 101, 11064–11069.
- Corcione, A., Aloisi, F., Serafini, B., Capello, E., Mancardi, G.L., Pistoia, V., Uccelli, A., 2005. B-cell differentiation in the CNS of patients with multiple sclerosis. *Autoimmun. Rev.* 4, 549–554.
- Craft, J.E., 2012. Follicular helper T cells in immunity and systemic autoimmunity. *Nat. Rev. Rheumatol.* 8, 337–347.
- Crotty, S., 2012. The 1-1-1 fallacy. *Immunol. Rev.* 247, 133–142.
- Cyster, J.G., 2003. Homing of antibody secreting cells. *Immunol. Rev.* 194, 48–60.
- Cyster, J.G., 2005. Chemokines, sphingosine-1-phosphate, and cell migration in secondary lymphoid organs. *Annu. Rev. Immunol.* 23, 127–159.
- Esen, N., Rainey-Barger, E.K., Huber, A.K., Blakely, P.K., Irani, D.N., 2014. Type-I interferon suppress microglial production of the lymphoid chemokine, CXCL13. *Glia* 62, 1452–1462.
- Finch, D.K., Ettinger, R., Karnell, J.L., Herbst, R., Sleeman, M.A., 2013. Effects of CXCL13 inhibition on lymphoid follicles in models of autoimmune disease. *Eur. J. Clin. Invest.* 43, 501–509.
- Fischer, L., Korfel, A., Pfeiffer, S., Kiewe, P., Volk, H.D., Cakiroglu, H., Widmann, T., Thiel, E., 2009. CXCL13 and CXCL12 in central nervous system lymphoma patients. *Clin. Cancer Res.* 15, 5968–5973.
- Fleming, J.O., Trousdale, M.D., el-Zaatari, F.A., Stohlman, S.A., Weiner, L.P., 1986. Pathogenicity of antigenic variants of murine coronavirus JHM selected with monoclonal antibodies. *J. Virol.* 58, 869–875.
- Forster, R., Mattis, A.E., Kremmer, E., Wolf, E., Brem, G., Lipp, M., 1996. A putative chemokine receptor, BLR1, directs B cell migration to defined lymphoid organs and specific anatomic compartments of the spleen. *Cell* 87, 1037–1047.
- Gelderblom, H., Londono, D., Bai, Y., Cabral, E.S., Quandt, J., Hornung, R., Martin, R., Marques, A., Cadavid, D., 2007. High production of CXCL13 in blood and brain during persistent infection with the relapsing fever spirochete *Borrelia turicatae*. *J. Neuropathol. Exp. Neurol.* 66, 208–217.
- Haas, J., Bekeredjian-Ding, I., Milkova, M., Balint, B., Schwarz, A., Korporal, M., Jarius, S., Fritz, B., Lorenz, H.M., Wildemann, B., 2011. B cells undergo unique compartmentalized redistribution in multiple sclerosis. *J. Autoimmun.* 37, 289–299.
- Hamo, L., Stohlman, S.A., Otto-Duessel, M., Bergmann, C.C., 2007. Distinct regulation of MHC molecule expression on astrocytes and microglia during viral encephalomyelitis. *Glia* 55, 1169–1177.

- Ireland, D.D., Stohlman, S.A., Hinton, D.R., Kapil, P., Silverman, R.H., Atkinson, R.A., Bergmann, C.C., 2009. RNase L mediated protection from virus induced demyelination. *PLoS Pathog.* 5, e1000602.
- Johanson, C.E., Duncan 3rd, J.A., Klinge, P.M., Brinker, T., Stopa, E.G., Silverberg, G.D., 2008. Multiplicity of cerebrospinal fluid functions: new challenges in health and disease. *Cerebrospinal Fluid Res.* 5, 10.
- Junt, T., Fink, K., Forster, R., Senn, B., Lipp, M., Muramatsu, M., Zinkernagel, R.M., Ludewig, B., Hengartner, H., 2005. CXCR5-dependent seeding of follicular niches by B and Th cells augments antiviral B cell responses. *J. Immunol.* 175, 7109–7116.
- Keim, C., Kazadi, D., Rothschild, G., Basu, U., 2013. Regulation of AID, the B-cell genome mutator. *Genes Dev.* 27, 1–17.
- Khademi, M., Kockum, I., Andersson, M.L., Iacobaeus, E., Brundin, L., Sellebjerg, F., Hillert, J., Piehl, F., Olsson, T., 2011. Cerebrospinal fluid CXCL13 in multiple sclerosis: a suggestive prognostic marker for the disease course. *Mult. Scler.* 17, 335–343.
- Kowarik, M.C., Cepok, S., Sellner, J., Grummel, V., Weber, M.S., Korn, T., Berthele, A., Hemmer, B., 2012. CXCL13 is the major determinant for B cell recruitment to the CSF during neuroinflammation. *J. Neuroinflammation* 9, 93.
- Krumbholz, M., Theil, D., Cepok, S., Hemmer, B., Kivisakk, P., Ransohoff, R.M., Hofbauer, M., Farina, C., Derfuss, T., Hartle, C., Newcombe, J., Hohlfeld, R., Meinl, E., 2006. Chemokines in multiple sclerosis: CXCL12 and CXCL13 up-regulation is differentially linked to CNS immune cell recruitment. *Brain: A J. Neurol.* 129, 200–211.
- Li, L., Narayan, K., Pak, E., Pachner, A.R., 2006. Intrathecal antibody production in a mouse model of Lyme neuroborreliosis. *J. Neuroimmunol.* 173, 56–68.
- Linterman, M.A., Beaton, L., Yu, D., Ramiscal, R.R., Srivastava, M., Hogan, J.J., Verma, N.K., Smyth, M.J., Rigby, R.J., Vinuesa, C.G., 2010. IL-21 acts directly on B cells to regulate Bcl-6 expression and germinal center responses. *J. Exp. Med.* 207, 353–363.
- Magliozzi, R., Columba-Cabezas, S., Serafini, B., Aloisi, F., 2004. Intracerebral expression of CXCL13 and BAFF is accompanied by formation of lymphoid follicle-like structures in the meninges of mice with relapsing experimental autoimmune encephalomyelitis. *J. Neuroimmunol.* 148, 11–23.
- Marques, C.P., Kapil, P., Hinton, D.R., Hindinger, C., Nutt, S.L., Ransohoff, R.M., Phares, T.W., Stohlman, S.A., Bergmann, C.C., 2011. CXCR3-dependent plasma blast migration to the central nervous system during viral encephalomyelitis. *J. Virol.* 85, 6136–6147.
- Maul, R.W., Gearhart, P.J., 2010. AID and somatic hypermutation. *Adv. Immunol.* 105, 159–191.
- Metcalfe, T.U., Baxter, V.K., Nilaratanakul, V., Griffin, D.E., 2013. Recruitment and retention of B cells in the central nervous system in response to alphavirus encephalomyelitis. *J. Virol.* 87, 2420–2429.
- Muramatsu, M., Kinoshita, K., Fagarasan, S., Yamada, S., Shinkai, Y., Honjo, T., 2000. Class switch recombination and hypermutation require activation-induced cytidine deaminase (AID), a potential RNA editing enzyme. *Cell* 102, 553–563.
- Okada, T., Cyster, J.G., 2006. B cell migration and interactions in the early phase of antibody responses. *Curr. Opin. Immunol.* 18, 278–285.
- Ozaki, K., Spolski, R., Feng, C.G., Qi, C.F., Cheng, J., Sher, A., Morse 3rd, H.C., Liu, C., Schwartzberg, P.L., Leonard, W.J., 2002. A critical role for IL-21 in regulating immunoglobulin production. *Science* 298, 1630–1634.
- Parker Harp, C.R., Archambault, A.S., Sim, J., Ferris, S.T., Mikesell, R.J., Koni, P.A., Shimoda, M., Lington, C., Russell, J.H., Wu, G.F., 2015. B cell antigen presentation is sufficient to drive neuroinflammation in an animal model of multiple sclerosis. *J. Immunol.* 194, 5077–5084.
- Phares, T.W., Ramakrishna, C., Parra, G.I., Epstein, A., Chen, L., Atkinson, R., Stohlman, S.A., Bergmann, C.C., 2009. Target-dependent B7–H1 regulation contributes to clearance of central nervous system infection and dampens morbidity. *J. Immunol.* 182, 5430–5438.
- Phares, T.W., Stohlman, S.A., Hinton, D.R., Atkinson, R., Bergmann, C.C., 2010. Enhanced antiviral T cell function in the absence of B7–H1 is insufficient to prevent persistence but exacerbates axonal bystander damage during viral encephalomyelitis. *J. Immunol.* 185, 5607–5618.
- Phares, T.W., Marques, C.P., Stohlman, S.A., Hinton, D.R., Bergmann, C.C., 2011. Factors supporting intrathecal humoral responses following viral encephalomyelitis. *J. Virol.* 85, 2589–2598.
- Phares, T.W., Stohlman, S.A., Hwang, M., Min, B., Hinton, D.R., Bergmann, C.C., 2012. CD4 T cells promote CD8 T cell immunity at the priming and effector site during viral encephalitis. *J. Virol.* 86, 2416–2427.
- Phares, T.W., Stohlman, S.A., Hinton, D.R., Bergmann, C.C., 2013. Astrocyte-derived CXCL10 drives accumulation of antibody-secreting cells in the central nervous system during viral encephalomyelitis. *J. Virol.* 87, 3382–3392.
- Phares, T.W., DiSano, K.D., Hinton, D.R., Hwang, M., Zajac, A.J., Stohlman, S.A., Bergmann, C.C., 2013. IL-21 optimizes T cell and humoral responses in the central nervous system during viral encephalitis. *J. Neuroimmunol.* 263, 43–54.
- Phares, T.W., DiSano, K.D., Stohlman, S.A., Bergmann, C.C., 2014. Progression from IgD+ IgM+ to isotype-switched B cells is site specific during coronavirus-induced encephalomyelitis. *J. Virol.* 88, 8853–8867.
- Ragheb, S., Li, Y., Simon, K., VanHaerents, S., Galimberti, D., De Riz, M., Fenoglio, C., Scarpini, E., Lisak, R., 2011. Multiple sclerosis: BAFF and CXCL13 in cerebrospinal fluid. *Mult. Scler.* 17, 819–829.
- Rainey-Barger, E.K., Rumble, J.M., Lalor, S.J., Esen, N., Segal, B.M., Irani, D.N., 2011. The lymphoid chemokine, CXCL13, is dispensable for the initial recruitment of B cells to the acutely inflamed central nervous system. *Brain Behav. Immun.* 25, 922–931.
- Ramakrishna, C., Bergmann, C.C., Atkinson, R., Stohlman, S.A., 2003. Control of central nervous system viral persistence by neutralizing antibody. *J. Virol.* 77, 4670–4678.
- Rankin, A.L., MacLeod, H., Keegan, S., Andreyeva, T., Lowe, L., Bloom, L., Collins, M., Nickerson-Nutter, C., Young, D., Guay, H., 2011. IL-21 receptor is critical for the development of memory B cell responses. *J. Immunol.* 186, 667–674.
- Rasheed, M.A., Latner, D.R., Aubert, R.D., Gourley, T., Spolski, R., Davis, C.W., Langley, W.A., Ha, S.J., Ye, L., Sarkar, S., Kalia, V., Konieczny, B.T., Leonard, W.J., Ahmed, R., 2013. IL-21 is a critical cytokine for the generation of virus-specific long-lived plasma cells. *J. Virol.*
- Reif, K., Ekland, E.H., Ohl, L., Nakano, H., Lipp, M., Forster, R., Cyster, J.G., 2002. Balanced responsiveness to chemoattractants from adjacent zones determines B-cell position. *Nature* 416, 94–99.
- Rubenstein, J.L., Wong, V.S., Kadoch, C., Gao, H.X., Barajas, R., Chen, L., Josephson, S.A., Scott, B., Douglas, V., Maiti, M., Kaplan, L.D., Treseler, P.A., Cha, S., Hwang, J.H., Cinque, P., Cyster, J.G., Lowell, C., 2013. CXCL13 plus interleukin 10 is highly specific for the diagnosis of CNS lymphoma. *Blood* 121, 4740–4748.
- Rupprecht, T.A., Plate, A., Adam, M., Wick, M., Kastenbauer, S., Schmidt, C., Klein, M., Pfister, H.W., Koedel, U., 2009. The chemokine CXCL13 is a key regulator of B cell recruitment to the cerebrospinal fluid in acute Lyme neuroborreliosis. *J. Neuroinflammation* 6, 42.
- Savarin, C., Stohlman, S.A., Atkinson, R., Ransohoff, R.M., Bergmann, C.C., 2010. Monocytes regulate T cell migration through the glia limitans during acute viral encephalitis. *J. Virol.* 84, 4878–4888.
- Scandella, E., Fink, K., Junt, T., Senn, B.M., Lattmann, E., Forster, R., Hengartner, H., Ludewig, B., 2007. Dendritic cell-independent B cell activation during acute virus infection: a role for early CCR7-driven B-T helper cell collaboration. *J. Immunol.* 178, 1468–1476.
- Tschen, S.I., Bergmann, C.C., Ramakrishna, C., Morales, S., Atkinson, R., Stohlman, S.A., 2002. Recruitment kinetics and composition of antibody-secreting cells within the central nervous system following viral encephalomyelitis. *J. Immunol.* 168, 2922–2929.
- Tschen, S.I., Stohlman, S.A., Ramakrishna, C., Hinton, D.R., Atkinson, R.D., Bergmann, C.C., 2006. CNS viral infection diverts homing of antibody-secreting cells from lymphoid organs to the CNS. *Eur. J. Immunol.* 36, 603–612.
- van Eijk, M., Defrance, T., Hennino, A., de Groot, C., 2001. Death-receptor contribution to the germinal-center reaction. *Trends Immunol.* 22, 677–682.
- Victoria, G.D., Nussenzweig, M.C., 2012. Germinal centers. *Annu. Rev. Immunol.* 30, 429–457.
- Wang, F.L., Hinton, D.R., Gilmore, W., Trousdale, M.D., Fleming, J.O., 1992. Sequential infection of glial cells by the murine hepatitis virus JHM strain (MHV-4) leads to a characteristic distribution of demyelination. *Lab. Invest.* 66, 744–754.
- Wengner, A.M., Hopken, U.E., Petrow, P.K., Hartmann, S., Schurigt, U., Brauer, R., Lipp, M., 2007. CXCR5- and CCR7-dependent lymphoid neogenesis in a murine model of chronic antigen-induced arthritis. *Arthritis Rheum.* 56, 3271–3283.
- Winter, S., Loddenkemper, C., Aebischer, A., Rabel, K., Hoffmann, K., Meyer, T.F., Lipp, M., Hopken, U.E., 2010. The chemokine receptor CXCR5 is pivotal for ectopic mucosa-associated lymphoid tissue neogenesis in chronic *Helicobacter pylori*-induced inflammation. *J. Mol. Med. (Berl.)* 88, 1169–1180.
- Yi, J.S., Cox, M.A., Zajac, A.J., 2010. Interleukin-21: a multifunctional regulator of immunity to infections. *Microbes Infect.* 12, 1111–1119.
- Zotos, D., Tarlinton, D.M., 2012. Determining germinal centre B cell fate. *Trends Immunol.* 33, 281–288.
- Zotos, D., Coquet, J.M., Zhang, Y., Light, A., D'Costa, K., Kallies, A., Corcoran, L.M., Godfrey, D.I., Toellner, K.M., Smyth, M.J., Nutt, S.L., Tarlinton, D.M., 2010. IL-21 regulates germinal center B cell differentiation and proliferation through a B cell-intrinsic mechanism. *J. Exp. Med.* 207, 365–378.